Bulletin of the Seismological Society of America, Vol. 102, No. 4, pp. 1850–1863, August 2012, doi: 10.1785/0120110297

Ⓔ

Seismicity within Arizona during the Deployment of the EarthScope USArray Transportable Array

by Jeffrey S. Lockridge, Matthew J. Fouch,* and J Ramón Arrowsmith

Abstract A detailed record of earthquake frequency and distribution is essential to understanding regional tectonic strain and seismic hazard, particularly in regions of low, but significant, seismicity levels. Comprehensive analyses of seismicity within Arizona have not been previously possible due to a lack of seismic stations in many regions, contributing to the perception that earthquakes within Arizona are rare and generally limited to the north-central and northwestern portions of the state. The EarthScope USArray Transportable Array (TA) was deployed within Arizona from April 2006 to March 2009 and provided the opportunity to examine seismicity on a statewide scale. In this study, we developed a streamlined workflow for producing a comprehensive earthquake catalog using TA data. We combined our new catalog with historical earthquake catalogs from several sources to produce the first comprehensive historical earthquake catalog for the state of Arizona. The TA-derived catalog is complete to local magnitude (M_L) ~ 1.2, contains crustal events as small as M_L 0.0, and includes events located within several previously unidentified areas of seismic activity in Arizona. We also identified 16 earthquake clusters, many of which have swarmlike behavior. These earthquake clusters account for 42% of the events identified during the study period, and they occur in all physiographic, geophysical, and tectonic settings. We suggest that swarms and clusters, such as those documented in this study, may represent an important mechanism for small-scale tectonic strain release within intraplate regions with otherwise apparently low seismicity levels.

Online Material: Figures comparing earthquake depth to physiographic province, elevation, crustal thickness, and heat flow; data tables including earthquake catalogs and velocity models; and an introductory User's Guide to the Antelope Environmental Data Collection Software suite.

Introduction

Western North America is a broad, active zone of deformation with well-documented seismic activity recorded from the plate boundary in the west to the Rocky Mountains in the east. Compared to the northern Basin and Range (Nevada), Wasatch Front (Utah), and the North America/Pacific plate boundary (California), much of Arizona has experienced low levels of recorded seismicity. Historically, the largest earthquakes and the majority of seismicity recorded within Arizona have been located in an area of north-central Arizona that has been described as the Northern Arizona Seismic Belt (NASB; Brumbaugh, 1987). However, historical seismicity is by no means limited to north-central Arizona. Earthquakes of M 4.0 or larger have been located throughout the Arizona Transition Zone (ATZ) and Basin and Range (BR) Provinces of Arizona, including an M_L 4.2 earthquake associated with a December 2003 swarm of twenty M_L 3.2 and larger earthquakes in eastern Arizona (Eagar and Fouch, 2007). In a study on the 1976 body magnitude (m_b) 4.9 earthquake in Chino Valley, a microseismicity rate of 0.3 events per day (Eberhart-Phillips *et al.*, 1981) was documented within the ATZ. Fault scarp analysis in the Santa Rita Mountains piedmont of southern Arizona has revealed significant slip during the mid-Pleistocene with an estimated seismic moment magnitude ranging from 6.4 to 7.3 (Pearthree and Calvo, 1987), which is similar in size to the 1887 M_w 7.4 earthquake in Sonora, Mexico (Natali and Sbar, 1982). Additionally, recurrence intervals ranging from 10 to 100 ky have been estimated for M ~ 7 sized events associated with normal faults throughout the southern BR province (Menges

*Now at the Department of Terrestrial Magnetism, Carnegie Institution of Washington, 5241 Broad Branch Road, NW, Washington, D.C. 20015.

and Pearthree, 1989). A key issue is that seismicity across the entire state has not yet been documented due to a paucity of seismic stations in most regions.

The deployment of the EarthScope USArray Transportable Array (TA; see the Data and Resources section) in Arizona from April 2006 to March 2009 (Fig. 1) provides the first opportunity to improve our understanding of the earthquake process and regional tectonic structure within Arizona. With station spacing of approximately 70 km and about 3 years of continuous recordings of three-component broadband seismic data, data from the TA enable us to document the frequency and geographical distribution of seismicity across Arizona for an extended period of time without a spatial sampling bias. In this study, we utilize TA data to develop the first statewide catalog of seismicity. The catalog is complete to $M_L \sim 1.2$ and reveals seismic activity throughout most of the state (Ⓔ see Table S1 in the electronic supplement to this paper). We combine this new catalog with existing earthquake catalogs to construct the first comprehensive historical earthquake catalog for Arizona (Ⓔ see Table S2). In this study, we find areas of spatial and temporal earthquake clustering in all three major physiographic provinces, suggesting that repeated slip along a single fault or series of proximate faults is a common occurrence regardless of tectonic and physiographic province. These findings are an important constraint for intraplate regions where small-scale seismicity may significantly contribute to tectonic strain release.

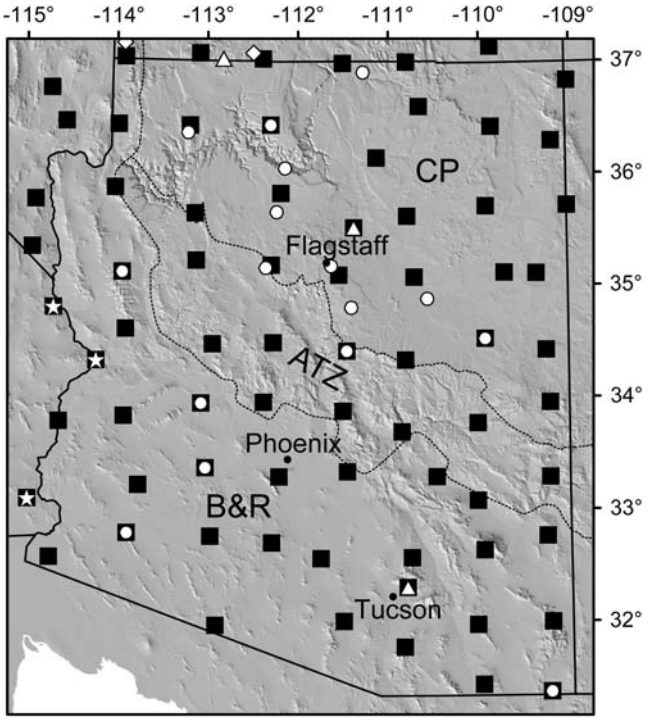

Figure 1. Seismic stations within Arizona used in this study. White shapes represent semipermanent seismic stations associated with the Northern Arizona Seismograph Network (AR, circles), Southern California Seismic Network (CI, stars), USGS (US, triangles), and Utah Seismograph Network (UU, diamonds). Solid black squares represent stations associated with the EarthScope USArray TA. Black squares with superimposed white shapes represent either preexisting stations that were included as part of the TA (stars and triangles) or TA stations adopted as part of the Arizona Integrated Broadband Network (circles). Boundaries between physiographic provinces (Colorado Plateau, CP; Arizona Transition Zone, ATZ; Basin and Range, BR) are denoted by dashed lines (see Peirce, 1984).

Historical Earthquake Catalogs

In an effort to fully characterize seismic activity within Arizona, we gathered historical earthquake data from multiple sources. The Advanced National Seismic System (ANSS) composite catalog is a worldwide earthquake catalog that contains a total of 813 unique Arizona events in the time window from 1935 to 2011 (see the Data and Resources section). Permanent networks contributing to this catalog include the National Earthquake Information Center, the Southern California Seismic Network, the Nevada Seismic Network, and the Utah Seismograph Network (Fig. 1). The Arizona Earthquake Information Center (AEIC) has compiled a regional catalog of historical events within Arizona dating back to 1830 containing 1004 unique events that were either recorded by the Northern Arizona Seismic Network (NASN; Fig. 1) or collected from previous earthquake catalogs (DuBois *et al.*, 1981; see the Data and Resources section). While earthquakes in the AEIC catalog that occurred before 1960 use hypocenter locations and event magnitudes estimated from felt reports and may not be accurate, the modern events have all been located using a crustal model modified from Warren (1969) (Brumbaugh, 1990; D. Brumbaugh, personal comm., 2011). Additional historical earthquakes not listed in the ANSS and AEIC catalogs include 12 events from the U.S. Geological Survey (USGS) Preliminary Determination of Epicenters (PDE) catalog (see the Data and Resources section) and events from local-scale seismic investigations (Kruger-Knuepfer *et al.*, 1985; Eagar and Fouch, 2007; Brumbaugh, 2008a,b).

These historical catalogs demonstrate clear spatial variations in seismicity across the state of Arizona (Fig. 2). First, the north-central portion of the state has been the most seismically active in terms of event frequency (Fig. 2b) and has produced the three largest historical earthquakes (M_L 6.0–6.2), all of which were located near Flagstaff, Arizona. These data form the basis for the most recent seismic hazard analysis for Arizona (Petersen *et al.*, 2008) and coincide with the location of the NASB, which has been proposed as the southwestern tectonic boundary of the Colorado Plateau (CP; Brumbaugh, 1987). The southwestern corner of Arizona is also an area of increased earthquake hazard due to its proximity to high seismicity rates in southern California and other regional earthquake activity. A few other areas are also characterized by relatively higher rates of historical seismicity. For instance, earthquakes near Lake Mead in northwestern Arizona may have been reservoir induced (Talwani,

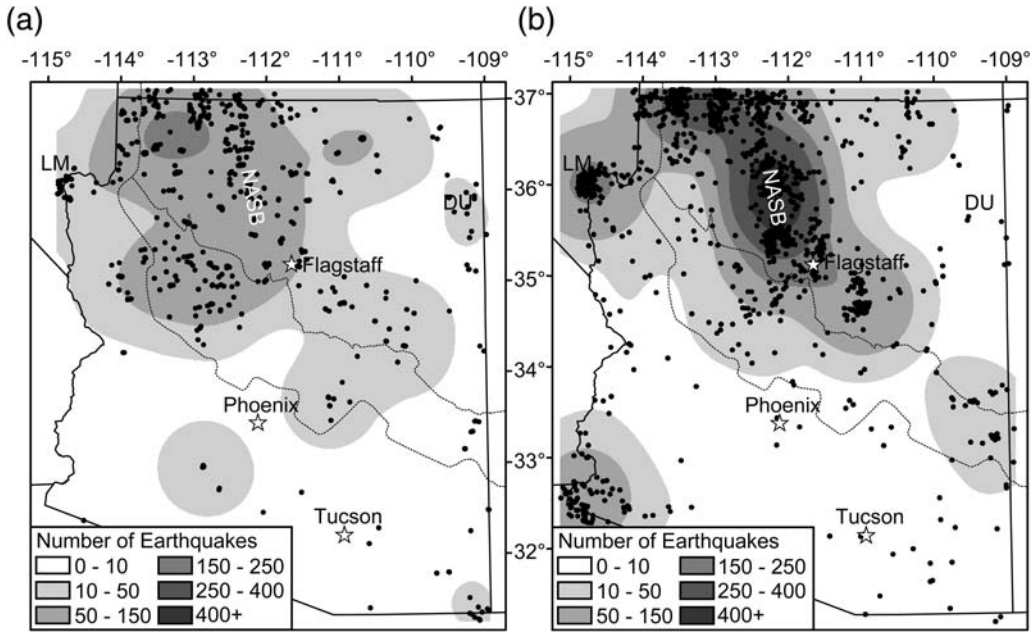

Figure 2. Density (shaded areas) and distribution of earthquakes (black dots) from modern and historical catalogs. In both (a) and (b), density is calculated as the cumulative events within a 100-km radius. (a) Earthquakes from this study recorded by USArray TA stations from April 2006 to March 2009. (b) Total historical events documented within Arizona from 1830 to 2011. Historical event data include the ANSS, AEIC, and USGS PDE catalogs, and selected references, which can be found in the Data and Resources section and the Ⓔ electronic supplement. Boundaries between physiographic provinces are the same as in Figure 1. The Defiance Uplift (DU) region, Lake Mead (LM), and NASB are labeled in both (a) and (b).

1997) or may be associated with active deformation within the Lake Mead fault system. Earthquakes along the Utah–Arizona border are likely to be the result of slip along a series of north–south trending normal faults (Pearthree *et al.*, 1983). Earthquake activity in southeastern Arizona corresponds to a region of seismicity extending from northeast Sonora, Mexico, into the Rio Grande Rift in New Mexico, some of which may be the result of continued activity from the 1887 M_w 7.4 Sonora earthquake (Castro *et al.*, 2010).

Despite the development of the ANSS and AEIC catalogs, the characterization of contemporary seismicity across the entire state of Arizona has been limited by a lack of comprehensive seismic station coverage. Prior to 1989, the few stations deployed within Arizona were mostly utilized for active source experiments and were not intended to record local earthquakes. Since 1989, however, a growing number of stations have been installed, including the semipermanent NASN stations located in the north-central portion of the state, permanent USGS-operated stations at Wupatki National Monument (WUAZ) and Tucson (TUC), and several stations along the California and Utah borders associated with other regional networks (Fig. 1). In addition to these permanent and semipermanent stations, several short-term regional arrays have been deployed within Arizona (e.g., COARSE, Frassetto *et al.* [2006]; LaRISTRA, Wilson *et al.* [2002]); however, these networks contribute little to the historical seismicity catalog, given their network design. This sparse and uneven distribution of stations across Arizona has created a sampling bias that has precluded a full characterization of the spatial distribution of seismicity for portions of the CP, ATZ, and southern BR.

Data and Methods

We evaluated data from the TA using the Antelope Environmental Data Collection Software suite (referred to as Antelope for the remainder of the paper; see the Data and Resources section) to construct an enhanced data analysis workflow that allows us to detect seismicity near the minimum level achievable given the TA station coverage. Our effort builds upon the initial work by the USArray Array Network Facility (ANF), which produces a catalog of events recorded at TA stations using a minimum of seven stations triggered to evaluate a potential event. The methods and workflow presented here are based in part on the ANF procedure and provide a template for the development of other regional earthquake catalogs using TA data or similar datasets.

Waveform data used in this study consisted of continuous 40 samples/s, three-component waveform data recorded at 92 USArray TA broadband seismometer stations located within or adjacent to the state of Arizona from April 2006 to March 2009 (Fig. 1; see also the Data and Resources section). Ⓔ A complete list of station names, locations, and network codes is provided in the electronic supplement (Table S3). As a courtesy to those who wish to follow the methodology described subsequently in this paper and generate a catalog using other regional datasets, we developed an

Antelope New User's Guide that introduces Antelope software functions and terminology. Ⓔ The Antelope guide is accompanied by sample Antelope parameter files and is available to be downloaded as part of the electronic supplement.

Automatic Event Detection and Initial Location

To detect and locate seismic events within Arizona over the duration of the dataset, we utilized Antelope's algorithms for automatic *P*-wave arrival detection (*dbdetect*), detection association (*dbgrassoc*), and hypocenter location (*dbgenloc*); see Pavlis *et al.* (2004). *Dbdetect* evaluates waveform data for potential seismic events by computing short-term average (STA) versus long-term average (LTA) ratios on one or more data channels, as specified by the user, and then flags instances where the specified detection parameters are satisfied as potential event arrivals. *Dbgrassoc* searches for families of arrivals determined from *dbdetect* that meet the required association criteria. These criteria may include the number of stations, maximum time range between the first and last arrival, and maximum station distance from the origin. *Dbgrassoc* then calls *dbgenloc*, which uses an iterative least-squares method that assigns weights to each arrival based on the residual time, an uncertainty value (if manually provided), and the distance from station to event to calculate an event hypocenter assuming the IASP91 velocity model (Kennett and Engdahl, 1991). Associated arrivals with hypocenters located outside of the study region are ignored by *dbgrassoc*.

To establish a travel time grid that extended just beyond the state borders, we used Antelope's *ttgrid* algorithm. For this study, we centered the grid at 34.2° N and –111.83° W and extended it 2.55° in the west–east direction and 2.95° in the north–south direction. For simplicity, we set the number of grid nodes to 151 in both directions, resulting in a grid spacing of ~1.9 km in the west–east direction and ~2.2 km in the north–south direction. The grid spacing is 2 km from the surface to 20 km depth, and 5 km from 20 to 55 km depth (Ⓔ see Fig. S1).

In an effort to calibrate *dbdetect* to detect the smallest events possible while minimizing spurious detections, we ran a series of tests with varying *dbdetect* parameter values to identify potential *P*-wave arrivals on vertical-component seismograms. Based on initial test runs using Antelope's default parameter file values, we confirmed that *dbdetect* was performing as expected by successfully identifying only potential *P*-wave arrivals. To fine-tune our ability to detect known *P* waves in the data, we altered specific parameters for *dbdetect*. We conclude that the best results were achieved with a signal-to-noise threshold of 3.5, an STA time window of 1.0, and an LTA time window of 5.0 (Ⓔ Antelope parameter files used in this study are available in the electronic supplement.)

We tested the efficacy of *dbgrassoc* for our study region by altering parameter values for (1) the main detection evaluation time window, (2) the evaluation time window step, and (3) the minimum number of station detections required for association. The initial testing was performed on a random cluster of events in the ATZ that occurred on 17 May 2008 in the vicinity of 34.35° N, –110.37° E. For these tests, we used station detection threshold values of 3, 4, and 5 without eliminating stations based on distance from the calculated hypocenter. A station threshold of 3 resulted in many false event detections, while a value of 5 resulted in the unsatisfactory exclusion of several smaller events. A station threshold of 4 resulted in the detection of 12 Arizona events, 9 out-of-state or spurious events, and 4 mine blasts for the 24-hour period tested. We then added a distance restriction to the station threshold value so that all stations greater than 1.5° from the calculated hypocenter were ignored. This addition resulted in the detection of 10 out of 12 Arizona events, 0 out-of-state or spurious events, and 5 mine blasts. We then examined a range of detection processing time window values (15, 20, 25, and 60 s) and concluded that 20 s was the optimal value because it detected the greatest number of earthquakes, while minimizing spurious events. Finally, we tested values for the frequency of detection processing of 5, 10, 15, and 40 s and concluded that 10 s was the optimal value for this parameter.

Once we established this satisfactory set of event association parameters, we applied the detection and event association algorithms to our dataset for all available data recorded in 2006. A cursory review of the first 1.5 months of data showed that these settings successfully identified most events in the ANF preliminary catalog, while including very few spurious events. Any events from the ANF catalog that were not detected were ignored by *dbgrassoc* because *dbdetect* had only found arrivals at three stations. We therefore concluded that the association algorithm was performing as expected.

To further test the detection and event association algorithm parameters, we examined a time window in which we had manually reviewed the waveform data for seismicity as part of a separate study of the Roosevelt Dam region, which is northeast of Phoenix and situated in the ATZ (Lockridge *et al.*, 2012). From 13:00 to 15:15 UTC on 25 June 2007, we visually detected and manually located 10 earthquakes adjacent to Roosevelt Lake. Of these 10 events, 2 were $M_L < 1.0$, 4 were $1.4 > M_L \geq 1.0$, and 4 were $M_L \geq 1.4$. The automatic detection and association algorithms successfully found all events with $M_L \geq 1.4$ but missed all events with $M_L < 1.4$. Through a visual review of the waveform data, we determined that *dbdetect* had successfully detected arrivals for all events with $M_L > 1.0$; however, *dbgrassoc* failed to associate these detections. We tested a series of signal-to-noise threshold values from 3.5 to 3.0 by increments of 0.1 and determined that changing this parameter did not improve associations for the smallest events. In another series of tests, we decreased the STA to LTA ratio value 1:5 to 0.5:4 and altered several other parameters, but in no case were we able to reduce the event detection threshold magnitude. Based on

these tests, we initially estimated that our methods were well tuned to detect and locate all local events with $M_L \geq 1.4$, as well as many with $M_L < 1.4$. However, this initial estimate is conservative, and we discuss our methods for determining earthquake magnitude and catalog completeness magnitude (M_c) in the Earthquake Relocation and Magnitude Calculation section.

Quality Control of Automatic Detection Processing

After applying the automatic detection and location algorithms to the entire dataset, we manually viewed the *P*-wave arrival times on vertical-component waveform data for each detected event using a 1 Hz high-pass filter. We classified events into four categories: local earthquake, mine or quarry blast, false or out-of-state event, and potential blast. In addition to the automatically detected events, we also manually reviewed a minimum of two hours of waveform data prior to and following larger earthquakes ($M_L \geq 2.0$) and during swarms to detect potential foreshocks and aftershocks that would be too small to be identified by the automatic detection algorithm.

We reviewed the initial catalog generated by the automated detection algorithm and found that, as expected, the detection of a small number of spurious events was unavoidable. These false detections were easily recognized by reviewing waveform data, because in each case the largest amplitude signals were not found on stations close to the hypocenter calculated by *dbgenloc* and waveforms were generally noisy with no clear *P* or *S* arrivals. Out-of-state earthquakes were also readily recognizable, because the nearest stations to the event hypocenters were located along the perimeters of the station grid. As expected, the majority of out-of-state events consisted of earthquakes in southern Utah, southern Nevada, and southeastern California, primarily along the San Andreas fault system in Baja, California. During this initial review, we removed all spurious and out-of-state events from the catalog.

Besides false detections and events located outside the boundaries of the study region, the majority of nonearthquake detections were mine and quarry blasts, an expected feature of the initial catalog given the broad range of mining and quarrying operations in the state. The reliability of the methods used for differentiating between human-generated blasts from mines and quarries and local earthquakes varies significantly from region to region (Baumgardt and Young, 1990) due to several factors, including blast type, location of blasts relative to the seismic network, station spacing, and other local conditions. Because crustal characteristics vary greatly between the three physiographic provinces in Arizona, we differentiated between human-generated blasts and local earthquakes on a case-by-case basis by performing (1) waveform character analysis and (2) a review of Google Earth satellite imagery in the areas of suspected blasts to assess the potential association with mines and quarries and other facilities that might generate blasts. Events with emergent or multiple *P* arrivals at all stations, long codas (25 s or more on stations within 1° of the event epicenter), and/or excessive low-frequency signals were classified as suspected mine blasts (Fig. 3; Stump *et al.*, 2002). For each

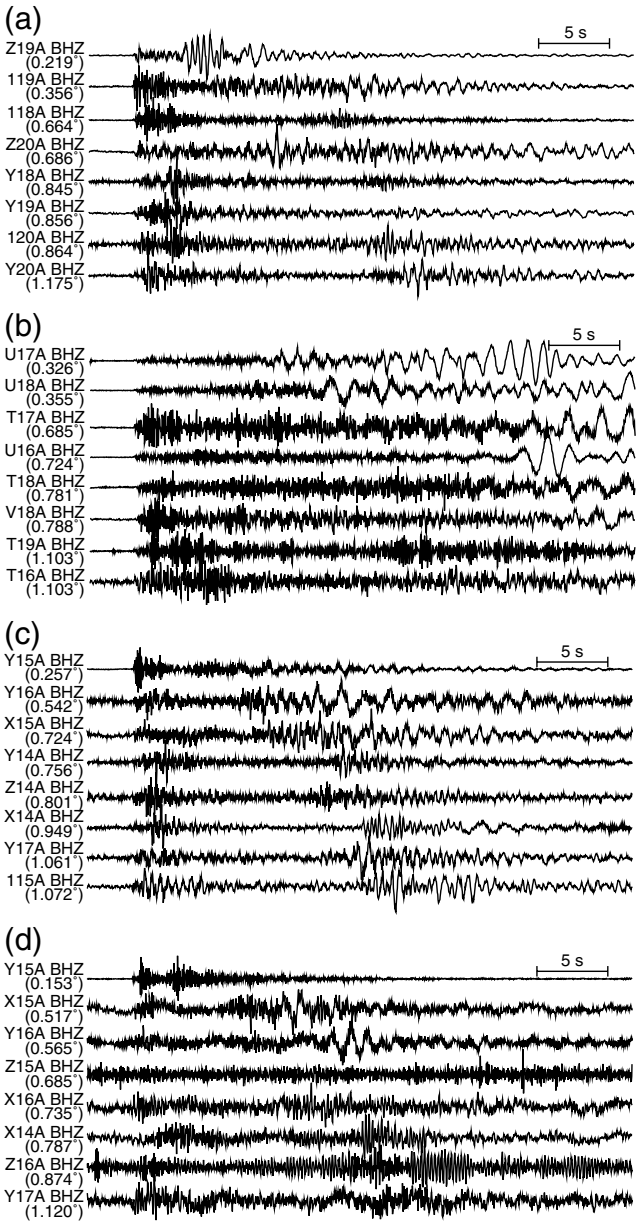

Figure 3. Record sections of typical human-generated blasts identified using automatic detection and location algorithms. Traces are vertical component, filtered at 1 Hz, and labeled with station names and distances from the source. (a) 3 August 2008 01:34:58 UTC blast at Morenci Copper Mine in southeastern Arizona. (b) 6 February 2008 20:39:17 UTC blast at Kayenta Coal Mine in northeastern Arizona. (c) 30 June 2008 23:12:48 UTC blast at a quarry site in the northern Phoenix metropolitan area. (d) 11 January 2008 16:27:30 UTC potential human-generated blast located north of Phoenix near New River. No evidence of human-generated blasting was observed near the New River event using Google satellite imagery; however, this event was flagged as potentially human-generated due to the emergent *P* and *S* arrivals and low frequency signal beyond 25 s on X15A and Y16A.

suspected blast, we compared the initial locations of these events with satellite imagery to create a list of active mine and quarry sites within Arizona (Ⓔ see Table S4). In many cases, blasts from individual mining and quarrying sites were distinctive enough that their source could be easily recognized based on waveform character alone. We flagged confirmed mine or quarry blasts in the Antelope event database and copied these events into a separate catalog (Ⓔ see Table S5). Because of the emergent nature of *P*-wave arrivals and the high volume of blasting events (10 or more within Arizona on weekdays), we consider the determination of accurate locations for most blasts beyond the scope of this study. Therefore, the final mine or quarry blast catalog produced in this study includes initial locations generated from the workflow described previously in this paper with no further analysis or quality control.

Events with waveform character similar to other blasts but not located near any known blasting locations or visibly scarred areas were flagged as potential human-generated seismic events and listed in a separate event catalog (Fig. 3; Ⓔsee Table S6). As with the confirmed blasts, potential human-generated blasts were difficult to locate. Therefore, data in Table S6 represents preliminary estimates of event origin times and locations. We identified 97 potential human-generated blasts during our period of study, 51 of which have initial location estimates within the BR province. The high rate of these events in the BR province suggests the possibility that earthquakes occurring within sedimentary basins have waveform characteristics similar to those of mine and quarry blasts. We suggest that this issue be further analyzed in future studies.

Earthquake Relocation and Magnitude Calculation

Following the completion of the automated detection and location procedure and the culling of nontectonic events including false detections and blasts, we manually reviewed waveform data for all tectonic events to provide more precise locations. We refined the initial *P* picks on the vertical component determined from *dbdetect*, and where clearly visible, we selected *S* waves on one of the horizontal components. Local earthquakes have distinctive waveform characteristics with impulsive *P*-wave arrivals that vary in amplitude according to azimuth, and a clearly identifiable *S* wave less than 20 s later on stations closer than 1° (Fig. 4). For each earthquake, we manually adjusted the *P* arrival picks originally assigned by *dbdetect*, picked *S*-wave arrivals on stations where the *S* phase was clear, and assigned time uncertainty values for each pick based on signal-to-noise values and the impulsiveness of the phase arrival. We used the initial hypocenter location to determine if the event was located within the CP, ATZ, or BR province and then selected the corresponding 1D regional velocity model (Ⓔ see Table S7; Warren [1969], Sinno *et al.* [1981]) to calculate the final hypocenter. To limit the number of events included in this study that may not be properly located because of our chosen

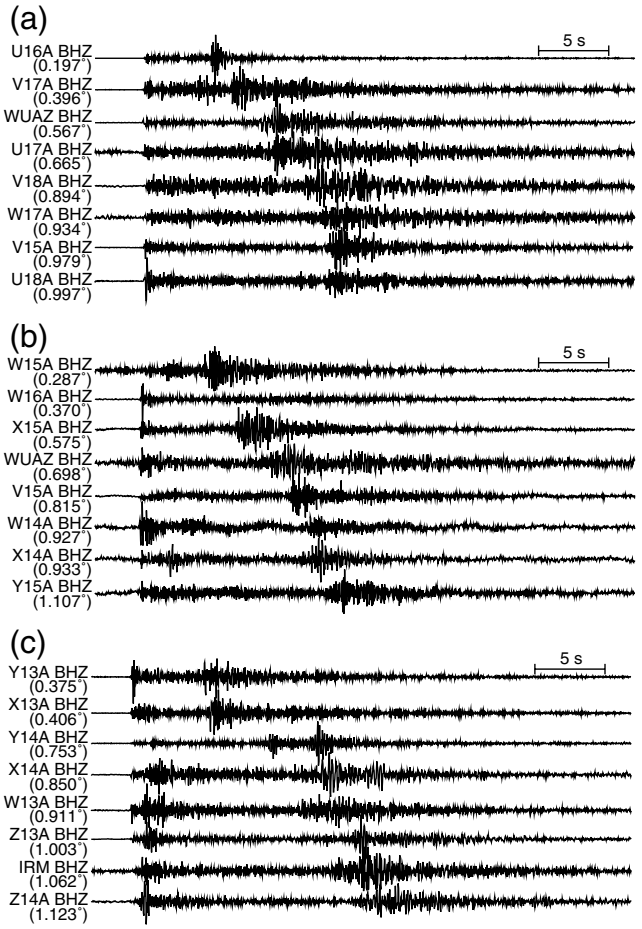

Figure 4. Record sections of waveform data for three earthquakes identified using automatic detection and location algorithms. Traces are vertical component, filtered at 1 Hz, and labeled with station names and distances from the hypocenter. (a) 2 August 2008 20:06:04 UTC M_L 1.8 earthquake located southeast of Tuba City within the CP. (b) 14 March 2008 03:40:56 UTC M_L 1.5 earthquake located northwest of Sedona within the ATZ. (c) 3 August 2008 09:53:23 UTC M_L 2.1 earthquake located east of Parker within the BR.

station distribution, we removed earthquakes located more than 0.1° from the Arizona state border from our final catalog.

As with all basic earthquake location methods, contributions from several sources can lead to errors in hypocentral locations. Major sources include station clock error, phase picking error, and an imperfect knowledge of the seismic wavespeed structure across the study region and locally beneath each station (e.g., significant basin structures, etc.). Station clock error for TA stations is very low (a few milliseconds at nearly all stations); we therefore do not consider this to be a significant source of error in our event locations. Picking errors are subjective, but given our strict criteria to select only those phases with sharp arrival onsets on waveforms with high signal-to-noise ratios, average picking errors for our dataset are <0.1 s. Conversely, the significant unknown variations in 3D crustal structure across the region make it

difficult to quantify the contribution to location errors. While the selection of regional 1D velocity models for each of the major geologic terranes helps to mitigate these errors, variations in regional crustal structure (e.g., Gilbert, 2012) will result in nonuniform errors across the entire study region. Overall, however, we believe that location errors may be systematic but are relatively small, given the fact that the average root mean square (rms) location error in our catalog is 0.10. Based on this rms value combined with previous analyses using this algorithm, we informally estimate epicentral distance errors of 2 km and depth errors of 5 km. Ⓔ We provide additional hypocenter location error information in the electronic supplement (Fig. S7).

We computed the M_L for each earthquake using Antelope's *orbevproc* program, which utilizes *mlrichter*, the standard local magnitude algorithm used for all USArray event data processing at the ANF. This is also the method used by the USGS to compute initial magnitudes. In this method, local magnitudes are computed using the methodology described by Richter (1935), which uses the largest three-component peak amplitude and applies an empirical scaling factor based on assumed attenuation at the event's epicentral distance. A small portion (6%) of the events in our catalog do not include magnitude information. These events are mostly characterized by few *P* and *S* arrivals, or signal-to-noise values near the detection threshold, suggesting very small M_L values.

To determine M_c and *b* values for our catalog, we compare the Gutenberg–Richter cumulative seismicity rate and earthquake magnitudes versus frequency (Fig. 5). Noting the range of potential values for the break in the curve of the Gutenberg–Richter cumulative seismicity rate plot, we performed a series of *b*-value calculations using magnitude minima starting at M_L 1.1 and increasing to M_L 1.6 by intervals of 0.1. We found that a cutoff of M_L 1.2 provided the best fit for the data, with an R^2 value of 0.9991 and a *b* value of 0.906 ± 0.017. We note that an M_c of 1.2 is a robust solution for this catalog, as it represents both the most reasonable break point in the Gutenberg–Richter cumulative seismicity rate curve and the maximum value of earthquake frequency as a function of magnitude (Fig. 5).

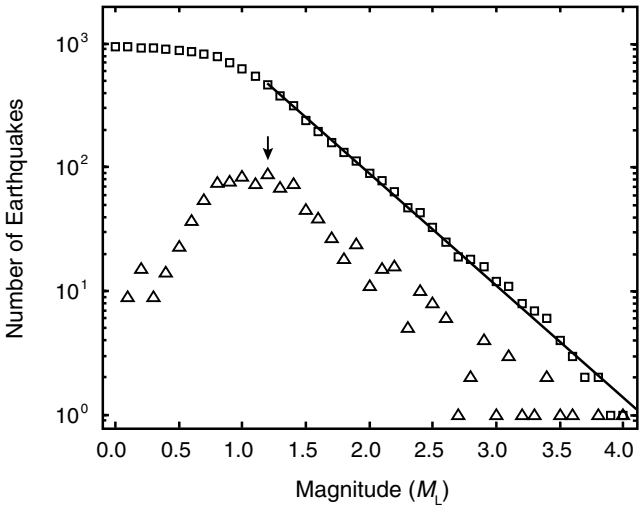

Figure 5. Earthquake magnitude frequency distribution of events located in this study. Triangles represent the total number of earthquakes for each magnitude; squares represent the cumulative number of earthquakes for a given magnitude and larger. The arrow highlights a M_c of M_L 1.2 for this catalog. The black line represents the best fit for the data ($R^2 = 0.9991$) using earthquakes with $M_L \geq 1.2$, which yields a *b* value of 0.906 ± 0.017 for this dataset.

Results

The primary results from this study are twofold. First, we developed the first comprehensive catalog by merging both the ANSS and AEIC catalogs, with a careful eye toward avoiding overlapping events from the two catalogs. The result of this effort yielded a new historical catalog for the state of Arizona with a total of 1961 unique events for the time period ranging from 1830 to 2011. Second, we identified and located a total of 995 earthquakes within or immediately adjacent to Arizona during the TA deployment from April 2006 to March 2009 (Ⓔ see Table S1). For the time period where TA station coverage in Arizona was most complete (April 2007–November 2008), we identified 884 earthquakes.

To provide an accurate comparison of our results with existing catalogs, we generated subsets of data for each catalog containing only events that occurred between 1 April 2007 and 30 November 2008 and were located within a 0.1° buffer outside the state borders of Arizona. Based on these parameters, the ANSS catalog contains 76 events, the AEIC catalog contains 4 events, and the ANF catalog contains 248 events. Our earthquake location effort identified all 4 AEIC events, 55 of the 76 ANSS events, and nearly all of the ANF events. We reviewed each of the 21 ANSS events not included in our catalog, and all except one were found to be human-generated seismic events, events with less than four stations within 1.5°, or events with weak *P*-wave arrivals that our autodetection algorithm did not flag. The one ANSS earthquake missed by our methods had *P* arrivals flagged on four stations within 1.4°, and it is unclear why it was not collected by the association algorithm. Of the 248 ANF events, we confirmed that all of the events were either included in our catalog or human-caused events that we excluded from our final catalog.

The new catalog represents a fourfold increase from the number of events found in the ANF catalog for the same time frame, with 884 events recorded while station coverage was most complete. Our analysis identified 292 events (29%) in the new catalog that were located at least 10 km from events recorded in historical earthquake catalogs. Notable areas of previously unidentified seismicity are located in the northwest portion of the ATZ, in the southeast corner of the state, and within the CP along the Arizona–New Mexico border (Fig. 2).

To calculate background seismicity rates within Arizona from April 2006 to March 2009, we performed a kernel density analysis of the event catalog using a search area radius of 1° (Fig. 2a). In general, seismic activity is most dense in the northwest quarter of the state, with a band of elevated seismicity extending to the southeast along the southern edge of the CP. Additionally, we detected elevated earthquake densities in the southeast corner of the state, as well as in portions of the interior of the CP. The maximum seismicity rate recorded during the TA deployment was 0.16 events within a 1° radius per day, which occurred in the northwest corner of the state between several swarms of repeating earthquakes. For comparison, we performed the same kernel density analysis on the cumulative historical earthquake catalog for Arizona (Fig. 2b) and found that historical earthquakes were most frequently recorded in the area of the NASB within the north-central portion of the state (Brumbaugh, 1987). This event distribution is also generally consistent with locations of known Quaternary active faults (see the Data and Resources section; Pearthree [1998], Pearthree and Bausch [1999]).

To analyze and map the depth distribution of events during the TA deployment, we utilized an inverse distance weighting interpolation (Watson and Philip, 1985) with a variable search radius using the nearest eight data points (Fig. 6a). This analysis revealed that while the majority of the state's seismicity occurred within the upper 20 km of the crust, areas of deeper seismicity were found along the Arizona–Utah border in northwest portion of the state, as well as the interior portions of the CP in the northeast portion of the state. Many events deeper than 20 km within the CP were scattered and adjacent to shallow events (< 20 km); however, we identified a zone containing 13 events ranging from 19 to 31 km in depth beneath the Defiance Uplift along the Arizona–New Mexico border in the northeast portion of the state. The Defiance Uplift region and the Arizona–Utah border in the northwestern portion of the state appear to be the only regions in Arizona that exhibit regular seismicity at depths exceeding 20 km. Additionally, seismicity within the ATZ is generally shallow compared to seismicity recorded within the BR province. To compare our results with historical data, we performed the same inverse distance weighting interpolation on the historical seismicity catalog (Fig. 6b) and found that the majority of historical earthquakes were shallow (< 20 km) with an average depth of 7.2 km. The historical catalogs include scattered deep (> 20 km) earthquakes throughout the state; however, aside from a swarm in eastern Arizona detected by Eagar and Fouch (2007), these deep earthquakes appear to be anomalous with no clear spatiotemporal patterns or association with physiographic or tectonic regime.

We performed additional analyses using earthquake depth recorded by the TA. Ⓔ Figure S2 shows histograms of hypocenter depth versus earthquake frequency for all of Arizona, as well as each of the three physiographic provinces of Arizona. The mean hypocenter depth of earthquakes within the CP was 12.5 km, which, as expected, is deeper than the average of 9.9 km for the state as a whole. However, despite higher elevations and thicker crust (e.g., Bashir *et al.*, 2011; Gilbert, 2012), the mean depth of earthquakes within the ATZ is 5.0 km, which is considerably shallower than the mean of 9.7 km found for the BR. We also searched for relationships or patterns between earthquake depth and elevation, crustal

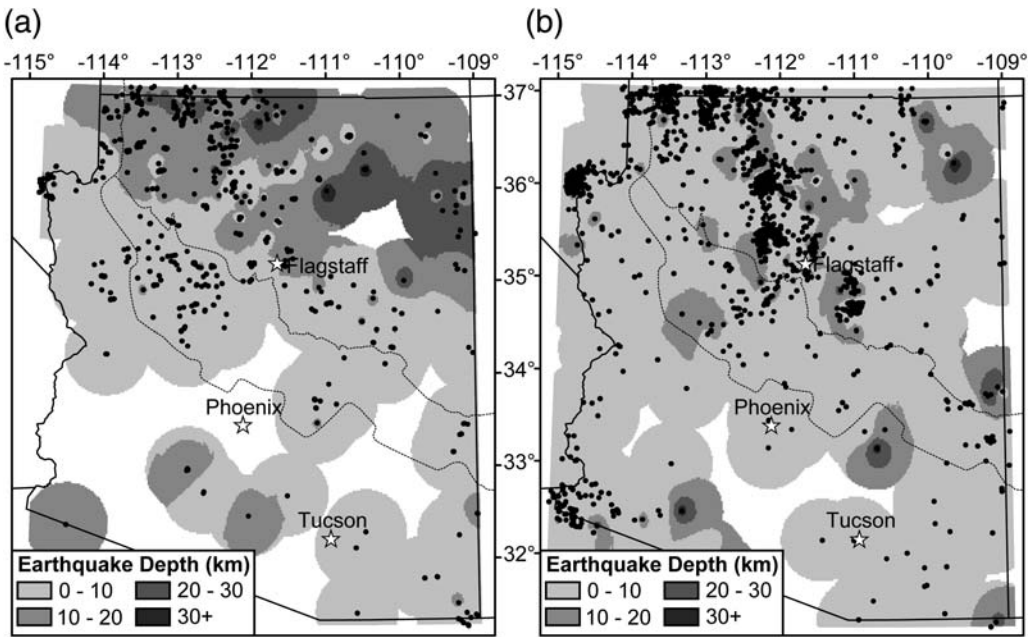

Figure 6. (a) Depth distribution of seismicity within Arizona during the TA deployment from April 2006 to March 2009. (b) Depth distribution of historical seismicity within Arizona from 1830 to 2011. Areas in white are located > 50 km from the nearest earthquake. Boundaries between physiographic provinces are the same as in Figure 1.

thickness, and heat flow. The range of earthquake depths generally increases in areas characterized by higher elevation, thicker crust, and low heat flow (Ⓔ see Figs. S3–S5). Because these properties are generally well correlated with one another, this is an expected result.

We note that while our catalog completeness magnitude is M_c 1.2, the vast majority of earthquakes recorded during the TA deployment were small in magnitude (91% with $M_L <$ 2.0 and 99% with $M_L < 3.0$). In an effort to determine the degree to which small-scale seismicity impacts overall seismic energy release across the state during TA deployment, we performed a series of calculations to convert M_L into seismic energy release (seismic moment, M_0). To examine moment release, we first converted the M_L values determined in our processing to moment magnitude (M_w):

$$M_w = [(1.5M_L + 16.0)/1.5] - 10.73.$$

We then converted M_w to M_0 using the empirical relationships described by Hanks and Kanamori (1979) and Lay and Wallace (1995):

$$\log M_0 = 1.5M_L + 16.0.$$

To examine the magnitude and spatial distribution of earthquake energy release throughout Arizona during the TA deployment, we computed the total seismic moment release from all earthquakes within 100 km of each event (Fig. 7a). This analysis reveals that the majority of the moment release occurred in the northwestern quarter of the state; however, we observe no other significant patterns or anomalies in the geographical distribution of cumulative moment release. We note several additional areas of elevated moment release scattered throughout the state; however, these regions are associated with isolated large earthquakes or multievent clusters. For the entire TA data study period, the total seismic moment was equivalent to a single event of approximately M_w 4.2. For comparison, we also performed an identical analysis on historical event data from 1959 to 2010 (Fig. 7b), which includes seven events with magnitudes ranging from M 5.0 to 5.75. The historical catalog also shows that the greatest moment release was in the northern portion of the state; however, this result is dominated by the larger events that occurred in the north-central portion of the state where historical seismic monitoring was most dense.

To highlight areas characterized by spatial clustering of earthquakes, we performed an earthquake density analysis with a search radius of 2 km and the cutoff for the number of events in a cluster set to 10. This analysis reveals a total of 16 locations where 10 or more earthquakes were located within a 2 km radius (Fig. 8). A total of 416 events, or 42% of our entire catalog, are associated with event clusters (Ⓔ see Table S8 for events associated with earthquake clusters and swarms). Of these 16 clusters, 10 were distinctly swarm-like (Fig. 9a,b), being characterized by temporal clustering (days to weeks) with the largest magnitude event not occurring as the first event in the sequence (two of the criteria

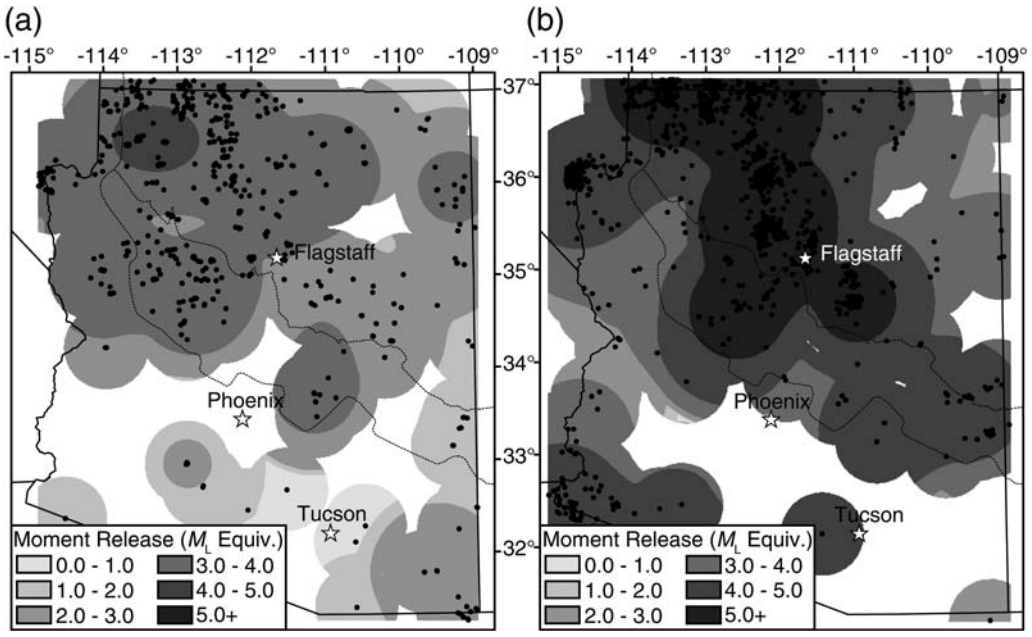

Figure 7. (a) Total seismic moment release (M_L equivalent) of earthquakes recorded by the TA from April 2006 to March 2009. (b) Total seismic moment of historical earthquakes from 1959 to 2011. Areas in white are located >50 km from the nearest earthquake. The three largest historical earthquakes located within Arizona were $M \sim 6.0+$ but are not included in this figure because they occurred in the early 1900s. Moment release per year calculations were not used in this figure, because the difference in time periods covered by the two datasets (3 vs. 50 years) is insufficient to account for the orders of magnitude difference in moment release between the two catalogs: the maximum magnitude event recorded for (a) was M_L 4.0 compared to a maximum of M_L 5.75 for (b), which includes 31 events of M_L 4.0 or greater.

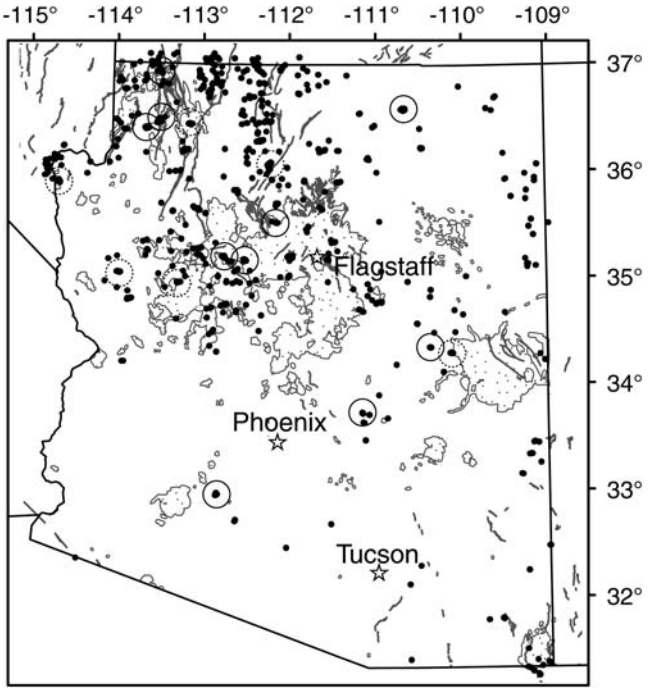

Figure 8. Location of swarms and clusters identified as part of this study compared to Quaternary faults within Arizona (dark gray lines; see the Data and Resources section) and post-15 m.y. volcanic outcrops in Arizona (filled areas; see Scarborough, 1985). Earthquakes recorded by USArray TA stations are depicted as black dots. Typical mainshock–aftershock type clusters are highlighted by dashed circles. Temporally clustered earthquake swarms are highlighted by solid circles.

specified by Vidale and Shearer, 2006). The remaining six clusters appeared to be typical mainshock–aftershock sequences, with the largest event at the beginning of the sequence (Fig. 9c).

Discussion

To first order, the new Arizona earthquake catalog is consistent with patterns in the historical catalog because the majority of the earthquakes occurred in the northwest portion of the state (Fig. 2). However, earthquakes in our catalog tend to be more evenly distributed, whereas the areas of highest earthquake density in the historical catalog are centered where historical seismic stations are most dense. To further illustrate this point, we note that the southwestern corner of Arizona has been historically well sampled by the regional Southern California Seismic Network, yet the entire Arizona–Mexico border is relatively poorly sampled in the USArray TA dataset because no stations lie south of the international border. Despite this difference, the historical catalog includes only three earthquakes in southwestern Arizona since the year 2000, so the presence of only one earthquake in our new catalog for this region is not surprising. Further, we detected multiple earthquakes in southeastern Arizona, suggesting that the Arizona–Mexico border was sufficiently sampled by our station distribution. These results

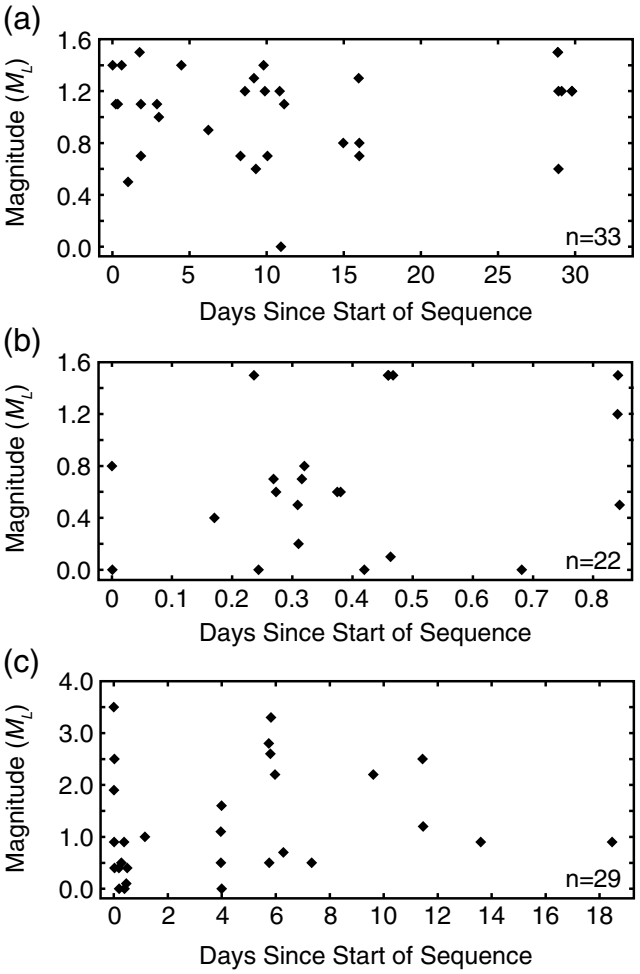

Figure 9. Event magnitude (M_L) distribution during three separate earthquake clusters identified as part of this study. (a) Earthquake swarm near the community of Shonto within the CP in northeastern Arizona. (b) Earthquake swarm near Gila Bend within the BR province in southwestern Arizona. (c) Earthquake cluster located within the Uinkaret Volcanic Field along the western margin of the CP in northwestern Arizona. Note that (a) and (b) are characteristic earthquake swarms with scattered temporal and magnitude distributions that occur regardless of swarm length. The Uinkaret cluster (c) is consistent with a series of mainshock–aftershock sequences characterized by a high frequency of small-magnitude events immediately following larger earthquakes. Note that the time axis represents the period of peak activity for each swarm or cluster. The number of events (n) recorded during the period of peak activity is given in the bottom right corner of each box and does not necessarily represent the total number of events associated with each swarm/cluster.

demonstrate that evenly distributed instrumentation is necessary to fully characterize seismic activity on a statewide scale, and suggest that longer-term recordings from USArray TA stations can improve earthquake hazard and regional seismicity rate determinations.

In our new catalog, the northwesternmost portion of the state and the central northeastern portion of the state are the only two regions where earthquake hypocenters were consistently located at depths greater than 20 km (Fig. 6a). It is

possible that these two regions of anomalously deep earthquakes are the result of inaccuracies in the local velocity models used to locate the events, whereby significant differences in crustal structure could account for mislocated events. However, the northwest portion of the state is characterized by 35–40 km thick crust (Brumbaugh, 1987; Bashir *et al.*, 2011; Gilbert, 2012), while the northeastern portion of the state is characterized by crust that is 40 km or greater in thickness (Gilbert *et al.*, 2007; Bashir *et al.*, 2011; Gilbert, 2012). In addition, both regions likely possess similar upper crustal velocities due to their similar compositions, suggesting that significant location error is not the cause of the inferred deep crustal seismicity. Further, earthquakes within both areas were located using the same crustal velocity model from Warren (1969) for the CP. The deeper earthquakes in the northwest portion of the state likely are associated with active fault systems, such as the Hurricane and Sevier–Toroweap faults that may penetrate to significant depths given their age and activity level (Fig. 8; Pearthree, 1998). In northeastern Arizona, events may be associated with crustal deformation due to the Defiance Uplift (Fig. 2), one of several monoclines within the CP. However, the Defiance region is believed to have been uplifted during the Laramide interval of the Late Cretaceous through Eocene time (Kelley, 1967), rendering this model unlikely. It is more likely that these deeper earthquakes are the result of an increased brittle–ductile transition depth due to the thicker regional crust and possible reactivation of preexisting structures.

The discrepancy between the average depths of earthquakes within the ATZ and BR provinces is potentially enhanced by the small number of events that occurred within the BR during our period of study. Additionally, 22 of the 50 events within the BR are associated with an earthquake sequence near Gila Bend in southern Arizona (Ⓔ see Table S8), which had an average depth of 13 km. When excluding the Gila Bend events from the calculation, the remaining 28 BR events have an average depth of 6.9 km, which is still deeper than the average depth of 5.0 km for the ATZ. Therefore, additional long-term monitoring of seismicity throughout Arizona is necessary to obtain a more definitive comparison of earthquake depths between physiographic provinces.

The 16 earthquake clusters identified as part of this study (Fig. 8) are groups of 10 or more earthquakes located within a 2 km radius and make up ~42% of the events recorded during the TA deployment in Arizona. Our manual review (see the Data and Methods section) of waveform data during swarms and clusters has had no effect on our determined M_c of 1.2, and it improves our catalog by including additional small-magnitude ($M_L < 1.2$) events that would have been otherwise missed by our automatic detection algorithm. However, this practice does have the potential to create a bias towards spatial clustering in the dataset because it may disproportionately increase the number of small-magnitude events ($M_L < 1.2$) found in the vicinity of larger events or swarms. To evaluate the potential bias towards spatial clustering, we compared the number of small-magnitude earthquakes ($M_L < 1.2$) to the number of larger earthquakes ($M_L \geq 1.2$). We find that 53% of the earthquakes in our catalog are $M_L < 1.2$. For events not associated with one of the 16 previously identified clusters, we find that 51% are $M_L < 1.2$, and for clustered events we find that 55% are $M_L < 1.2$. While it is likely that the manual review processing component of our workflow is responsible for the slight increase (~4%) in small-magnitude earthquake occurrence from nonclustered to clustered events, it does not appear to have artificially inflated the number of clusters or the overall percentage of clustered events in our catalog.

We also observe no correlation between physiographic or geologic setting and cluster location, as clusters occur in all regions of Arizona. Clusters in northwestern Arizona appear to be associated with areas of documented Quaternary faulting (Fig. 8; Menges and Pearthree [1983], Pearthree [1998], Pearthree and Bausch [1999]); however, several clusters are also located within areas of recent (< 15 Ma) volcanic activity (Fig. 8). We also identified a cluster within a sedimentary basin near the town of Gila Bend in southern Arizona. Two clusters were located adjacent to the man-made reservoirs of Lake Mead and Theodore Roosevelt Lake; however, studies of seismicity near these reservoirs did not find a correlation between seismic activity and reservoir water levels (Rogers and Lee, 1976; Lockridge *et al.*, 2012).

Additionally, we defined a swarm as a spatially clustered event group that exhibits a significant degree of temporal clustering with no obvious mainshock at the start of the sequence. In some cases, more than 20 events were identified on the same day, with as many as 49 events occurring within a one-week period. Earthquakes associated with a given swarm displayed remarkably similar waveform character to one another, suggesting that most of the swarms occur as a result of repeating slip along a single fault plane (Ⓔ see Fig. S6 in the electronic supplement; Lockridge *et al.*, 2012). A detailed analysis of each swarm is beyond the scope of the present study. Here we comment on the tectonic and physiographic setting of these earthquake clusters and the significance of their widespread occurrence.

Of the 16 earthquake clusters, 10 were relatively swarm-like, with temporal clustering ranging from days to weeks and the largest event not occurring as the first event in the sequence (Vidale and Shearer, 2006). In addition to the earthquake swarms identified as part of this study, state historical swarms have been identified in eastern Arizona (Eagar and Fouch, 2007), near Fredonia (Kruger-Knuepfer *et al.*, 1985), and in the San Francisco volcanic field (see the Data and Resources section).

Most studies associated with earthquake swarms point to the migration of hydrothermal fluids (Heinike *et al.*, 2009), fluid injection (Frohlich *et al.*, 2011), or magma injection (Špičák, 2000; Kurz *et al.*, 2004) as their cause; however, the occurrence of swarms has also been attributed to aseismic slip in both subduction zone (Holtkamp and

Brudzinski, 2011) and transform fault (Vidale and Shearer, 2006) environments. Other areas with intraplate swarms that may or may not be associated with fluid migration include Arkansas (Rabak *et al.*, 2010) and Ontario, Canada (Ma and Eaton, 2009). In most studies of seismic swarms, the largest event in the swarm sequence is $M \geq 4.0$; however, only four of the swarms identified in the current study contain events larger than M_L 3.0. This might suggest that within regions of low seismic activity, tectonic strain commonly may be accommodated by repeated small-magnitude events or swarmlike earthquake sequences, in addition to occasional moderate earthquakes and infrequent large earthquakes. We also note that it is likely that future TA-based seismicity studies will provide ample opportunity to examine this phenomenon in multiple tectonic and physiographic environments as the TA continues its eastward migration.

While this type of study is useful for developing new earthquake catalogs and discovering areas of previously unidentified seismic activity, it remains difficult to generate fault-plane solutions for most of these events due to their small magnitude (97% are $M_L \leq 2.5$). As part of a concurrent study, we analyzed a series of earthquakes that occurred in June 2007 near Theodore Roosevelt Lake, ~130 km northeast of Phoenix (Lockridge *et al.*, 2012). In that study, we determined focal mechanisms for the two largest events (M_L 2.7 and M_L 3.1) that were consistent with slip along a northwest–southeast trending normal fault located nearby. This cluster, along with several events near Lake Mead in the northwest portion of the state (Rogers and Lee, 1976), and the 4 February 1976 m_b 4.9 Chino Valley earthquake (Eberhart-Phillips *et al.*, 1981) represent the only historical Arizona earthquakes outside of the southwestern margin of the CP province for which fault-plane solutions have been calculated. Future work should include the determination of focal mechanisms for the larger events and perhaps clusters of small-magnitude repeating events in an effort to (1) further characterize the state of tectonic stress within portions of Arizona where focal mechanism solutions are not well studied (i.e., the interior of the CP and BR provinces) and (2) provide additional context to better understand the tectonic evolution of the CP, an active topic of discussion (e.g., Karlstrom *et al.*, 2008; Roy *et al.*, 2009; Crow *et al.*, 2011; Levander *et al.*, 2011; Wernicke, 2011).

Further, three years of data from the USArray TA deployment within Arizona is insufficient to fully characterize the moment release and earthquake hazard within the region. In more tectonically active regions such as southern California or other plate boundaries, tectonic strain rates are high, and therefore the earthquake cycle is relatively short and can be effectively monitored over a period of years to decades. In Arizona, recurrence intervals for $M \sim 7$ earthquakes associated with normal faults throughout the southern BR province are estimated to range from 10 to 100 ky (Menges and Pearthree, 1989). We conclude that the deployment of additional stations and the development of a statewide long-term regional network would be necessary to capture a broader range of the earthquake cycle to improve estimated rates of seismicity and hazard for the entire state of Arizona.

Conclusions

We developed a workflow to effectively and efficiently process waveform data from a regional broadband seismometer array with station spacing similar to that of the USArray TA (~70 km), and to produce a catalog of seismicity complete to M_L 1.2 for the state of Arizona. This study serves as a template for future TA-based and other regional studies with similar experiment configurations. In the state of Arizona, spatial coverage of the TA led to the identification of seismicity within areas previously thought to be tectonically inactive relative to neighboring states. Of the 995 events contained in our new catalog, we identified 292 (29%) located at least 10 km away from events recorded in historical earthquake catalogs, and we identified 579 (58%) events located at least 10 km from documented Quaternary faults. The most notable areas of previously unidentified seismicity are located in the northwest portion of the ATZ, in the southeastern corner of the state, and within the CP along the Arizona–New Mexico border. We found that the majority of the events that occur within Arizona are shallow (< 20 km). We also identified 16 clusters of 10 or more earthquakes within a 2 km radius. Of these 16 clusters, we noted 10 with swarmlike characteristics, chiefly, (1) temporal clustering over a period of days to weeks and (2) the largest magnitude event occurring somewhere in the middle of the temporal sequence.

This study confirms that broad, uniformly spaced seismometer station locations and coverage area have a significant impact on measured seismicity rates and hazard analysis for a given region. Further, the presence of regional seismicity, as well as earthquake swarms and clusters, in all three physiographic provinces of Arizona suggests that spatiotemporal earthquake clustering may be a significant mechanism of regional strain release regardless of tectonic or physiographic setting. More broadly, our study suggests that small-scale tectonic strain within continental interiors can be accommodated through small-magnitude earthquakes.

Data and Resources

The USArray Array Network Facility (ANF) provided data for this study in the form of a database for the Antelope Environmental Data Collection Software suite (http://www.brtt.com, last accessed May 2011). Historical earthquake data for this study was collected from the Advanced National Seismic System (ANSS) composite catalog at http://www.ncedc.org/cnss/catalog-search.html (last accessed May 2011), Arizona Earthquake Information Center (AEIC) catalog at http://www.cefns.nau.edu/Orgs/aeic/eq_history.html (last accessed April 2011), U. S. Geological Survey (USGS) National Earthquake Information Center (NEIC) Preliminary Determination of Epicenters (PDE) catalog (http://earthquake

.usgs.gov/earthquakes/eqarchives/epic/, last accessed May 2011), and selected papers referenced in the text. Preliminary event data recorded by the EarthScope USArray Transportable Array (http://earthscope.org/usarray, last accessed May 2011) was obtained from the EarthScope ANF website http://anf.ucsd.edu/tools/events/download.php (last accessed June 2011). Quaternary fault data was obtained from the USGS Quaternary Fault and Fold Database for the United States at http://earthquake.usgs.gov/hazards/qfaults (last accessed June 2011) and http://repository.usgin.org/uri_gin/usgin/dlio/317 (last accessed May 2011).

Acknowledgments

We thank Kevin Eagar and Jennifer Eakins for passing along their Antelope software knowledge, the EarthScope USArray Transportable Array team for installing and maintaining the stations used for this study, the Incorporated Research Institutions for Seismology (IRIS) Data Management Center for providing waveforms, and Frank Vernon and others of the USArray Array Network Facility (ANF) team for providing the initial Antelope database that allowed us to efficiently initiate this study. We would also like to thank Lisa Linville, Jeri Young, Phil Pearthree, David Brumbaugh, and Susan Beck for productive discussions, earthquake data, and reference materials. This work was supported by the Arizona Geological Survey and the Arizona Department of Emergency Management via a grant from the Federal Emergency Management Agency, and by the National Science Foundation via an EarthScope Science CAREER grant to M. J. Fouch (EAR-0548288).

References

Bashir, L., S. S. Gao, K. H. Liu, and K. Mickus (2011). Crustal structure and evolution beneath the Colorado Plateau and the southern Basin and Range Province: Results from receiver function and gravity studies, *Geochem. Geophys. Geosys.* **12,** Q06008.

Baumgardt, D. R., and G. B. Young (1990). Regional seismic waveform discriminants and case-based event identification using regional arrays, *Bull. Seismol. Soc. Am.* **80,** 1874–1892.

Brumbaugh, D. S. (1987). A tectonic boundary for the southern Colorado plateau, *Tectonophysics* **136,** 125–136.

Brumbaugh, D. S. (1990). Depth of the Fredonia, Arizona, earthquakes of 15 February 1962, *Bull. Seismol. Soc. Am.* **80,** 1762–1764.

Brumbaugh, D. S. (2008a). Seismicity and tectonics of the Blue Ridge area of the Mogollon Plateau, Arizona, *Bull. Seismol. Soc. Am.* **98,** 1527–1534.

Brumbaugh, D. S. (2008b). Seismicity and active faulting of the Kanab-Fredonia area of the southern Colorado Plateau, *J. Geophys. Res.* **113,** no. B05309, 9, doi 10.1029/2007JB005278.

Castro, R. R., P. M. Shearer, L. Astiz, M. Suter, C. Jacques-Ayala, and F. Vernon (2010). The long-lasting aftershock series of the 3 May 1887 M_w 7.5 Sonora earthquake in the Mexican Basin and Range Province, *Bull. Seismol. Soc. Am.* **100,** 1153–1164.

Crow, R., K. Karlstrom, Y. Asmerom, B. Schmandt, V. Polyak, and S. A. DuFrane (2011). Shrinking of the Colorado Plateau via lithospheric mantle erosion: Evidence from Nd and Sr isotopes and geochronology of Neogene basalts, *Geology* **39,** 27–30.

DuBois, S. M., M. L. Sbar, and T. A. Nowak (1981). Historical seismicity in Arizona, *Ariz. Bur. Geol. Min. Tech. Open-File Rept. 82-2*, 199 pp.

Eagar, K. C., and M. J. Fouch (2007). Detection of a unique earthquake swarm in eastern Arizona, *Arizona Geol.* **37,** 1–5.

Eberhart-Phillips, D., R. M. Richardson, M. L. Sbar, and R. B. Hermann (1981). Analysis of the 4 February 1976 Chino Valley, Arizona, earthquake, *Bull. Seismol. Soc. Am.* **71,** 787–801.

Frassetto, A., H. Gilbert, G. Zandt, S. Beck, and M. J. Fouch (2006). Support of high elevation in the southern Basin and Range based on the composition and architecture of the crust in the Basin and Range and Colorado Plateau, *Earth Planet. Sci. Lett.* **249,** 62–73.

Frohlich, C., C. Hayward, B. Stump, and E. Potter (2011). The Dallas–Fort Worth earthquake sequence: October 2008 through May 2009, *Bull. Seismol. Soc. Am.* **101,** 327–340.

Gilbert, H. (2012). Crustal structure and signatures of recent tectonism as influenced by ancient terranes in the western United States, *Geosphere* **8,** 141–157.

Gilbert, H., A. A. Velasco, and G. Zandt (2007). Preservation of Proterozoic terrane boundaries within the Colorado Plateau and implications for its tectonic evolution, *Earth Planet. Sci. Lett.* **258,** 237–248.

Hanks, T. C., and H. Kanamori (1979). A moment-magnitude scale, *J. Geophys. Res.* **84,** 2348–2350.

Heinicke, J., T. Fischer, R. Gaupp, J. Götze, U. Koch, H. Konietzky, and K.-P. Stanek (2009). Hydrothermal alteration as a trigger mechanism for earthquake swarms: The Vogtland/NW Bohemia region as a case study, *Geophys. J. Int.* **178,** 1–13.

Holtkamp, S. G., and M. R. Brudzinski (2011). Earthquake swarms in circum-Pacific subduction zones, *Earth Planet. Sci. Lett.* **305,** 215–225.

Karlstrom, K., R. Crow, L. Crossey, D. Coblentz, and J. Van Wijk (2008). Model for tectonically driven incision of the younger than 6 Ma Grand Canyon, *Geology* **36,** 835–838.

Kelley, V. C. (1967). Tectonics of the Zuni-Defiance region, New Mexico and Arizona, in *Guidebook of Defiance–Zuni–Mt. Taylor Region, Arizona and New Mexico: New Mexico Geological Society, Guidebook 18*, F. D. Trauger (Editor), New Mexico Geological Society, Socorro, New Mexico, 28–31.

Kennett, B. L. N., and E. R. Engdahl (1991). Traveltimes for global earthquake location and phase identification, *Geophys. J. Int.* **105,** 429–465.

Kruger-Knuepfer, J. L., M. L. Sbar, and R. M. Richardson (1985). Microseismicity of the Kaibab Plateau, northern Arizona, and its tectonic implications, *Bull. Seismol. Soc. Am.* **75,** 491–506.

Kurz, J. H., T. Jahr, and G. Jentzsch (2004). Earthquake swarm examples and a look at the generation mechanism of the Vogtland/Western Bohemia earthquake swarms, *Phys. Earth Planet. In.* **142,** 75–88.

Lay, T., and T. C. Wallace (1995). *Modern Global Seismology*, Academic Press, New York, 521 pp.

Levander, A., B. Schmandt, M. S. Miller, K. Liu, K. E. Karlstrom, R. S. Crow, C.-T. A. Lee, and E. D. Humphreys (2011). Continuing Colorado plateau uplift by delamination-style convective lithospheric downwelling, *Nature* **472,** 461–465.

Lockridge, J. S., M. J. Fouch, J R. Arrowsmith, and L. Linkimer (2012). Analysis of seismic activity near Theodore Roosevelt Dam, Arizona, during the occupation of the EarthScope/USArray transportable array, *Seismol. Res. Lett.* (in press).

Ma, S., and D. W. Eaton (2009). Anatomy of a small earthquake swarm in southern Ontario, Canada, *Seismol. Res. Lett.* **80,** 214–223.

Menges, C. M., and P. A. Pearthree (1983). Map of neotectonic deformation in Arizona, *Ariz. Bur. Geol. Min. Tech. Open-File Rept. 83-22*, scale 1:500,000.

Menges, C. M., and P. A. Pearthree (1989). Late Cenozoic tectonism in Arizona and its impact on regional landscape evolution, in Geologic Evolution of Arizona, *Arizona Geol. Soc. Digest* **17,** 649–680.

Natali, S. G., and M. L. Sbar (1982). Seismicity in the epicentral region of the 1887 northeastern Sonoran earthquake, Mexico, *Bull. Seismol. Soc. Am.* **72,** 181–196.

Pavlis, G. L., F. Vernon, D. Harvey, and D. Quinlan (2004). The generalized earthquake-location (GENLOC) package: An earthquake-location library, *Comput. Geosci.* **30,** 1079–1091.

Pearthree, P. A. (1998). Quaternary fault data and map for Arizona, *Arizona Geol. Surv. Open-File Rept. 98-24*, 122 pp., scale 1:750,000, 1 disk.

Pearthree, P. A., and D. B. Bausch (1999). Earthquake hazards in Arizona, *Arizona Geol. Survey Map 34*, scale 1:1,000,000.

Pearthree, P. A., and S. S. Calvo (1987). The Santa Rita fault zone: Evidence for large magnitude earthquakes with very long recurrence intervals,

basin and range province of southeastern Arizona, *Bull. Seismol. Soc. Am.* **77,** 97–116.

Pearthree, P. A., C. M. Menges, and L. Mayer (1983). Distribution, recurrence, and possible tectonic implications of late Quaternary faulting in Arizona, *Ariz. Bur. Geol. Min. Tech. Open-File Rept. 83.20*, p. 36.

Peirce, H. W. (1984). The Mogollon escarpment, *Ariz. Bur. Geol. Min. Tech., Fieldnotes* **4,** no. 2, 8–11.

Petersen, M. D., A. D. Frankel, S. C. Harmsen, C. S. Mueller, K. M. Haller, R. L. Wheeler, R. L. Wesson, Y. Zeng, O. S. Boyd, D. M. Perkins, N. Luco, E. H. Field, C. J. Wills, and K. S. Rukstales (2008). Documentation for the 2008 update of the United States national seismic hazard maps, *U. S. Geol. Surv. Open-File Rept. 2008–1128*.

Rabak, I., C. Langston, P. Bodin, S. Horton, M. Withers, and C. Powell (2010). The Enola, Arkansas, intraplate swarm of 2001, *Seismol. Res. Lett.* **81,** 549–559.

Richter, C. F. (1935). An instrumental earthquake magnitude scale, *Bull. Seismol. Soc. Am.* **25,** 1–32.

Rogers, A. M., and W. H. K. Lee (1976). Seismic study of earthquakes in the Lake Mead, Nevada-Arizona region, *Bull. Seismol. Soc. Am.* **66,** 1657–1681.

Roy, M., T. H. Jordan, and J. Pederson (2009). Colorado Plateau magmatism and uplift by warming of heterogeneous lithosphere, *Nature* **459,** 978–982.

Scarborough, R. B. (1985). Map of post-15-m.y. volcanic outcrops in Arizona, *Ariz. Bur. Geol. Min. Tech., Geol. Surv. Branch Map 21*, scale 1:1,000,000.

Sinno, Y. A., G. R. Keller, and M. L. Sbar (1981). A crustal seismic refraction study in west-central Arizona, *J. Geophys. Res.* **86,** 5023–5038.

Špičák, A. (2000). Earthquake swarms and accompanying phenomena in intraplate regions: A review, *Studia Geophys. Geod.* **44,** 89–106.

Stump, B. W., M. A. H. Hedlin, D. C. Pearson, and V. Hsu (2002). Characterization of mining explosions at regional distances: Implications with the International Monitoring System, *Rev. Geophys.* **40,** p. 1011.

Talwani, P. (1997). On the nature of reservoir induced seismicity, *Pure Appl. Geophys.* **150,** 473–492.

Vidale, J. E., and P. M. Shearer (2006). A survey of 71 earthquake bursts across southern California: Exploring the role of pore fluid pressure fluctuations and aseismic slip as drivers, *J. Geophys. Res.* **111,** no. B05312, 12, doi 10.1029/2005JB004034.

Warren, D. H. (1969). A seismic refraction survey of crustal structure in central Arizona, *Geol. Soc. Am. Bull.* **80,** 257–282.

Watson, D. F., and G. M. Philip (1985). A refinement of inverse distance weighted interpolation, *Geo. Process.* **2,** 315–327.

Wernicke, B. (2011). The California River and its role in carving Grand Canyon, *Geol. Soc. Am. Bull.* **123,** 1288–1316.

Wilson, D., J. Leon, R. Aster, J. Ni, J. Schlue, S. Grand, S. Semken, S. Baldridge, and W. Gao (2002). Broadband seismic background noise at temporary seismic stations observed on a regional scale in the southwestern United States, *Bull. Seismol. Soc. Am.* **92,** 3335–3342.

School of Earth and Space Exploration
Arizona State University
P.O. Box 871404
Tempe, Arizona 85287-1404
Lockridge@asu.edu

Manuscript received 17 October 2011